BEHAVIOUR OF A NEW TYPE OF COMPOSITE CONNECTION

Szilvia Erdélyi and László Dunai

HAS-BUTE Research Group for Computational Structural Mechanics
Department of Structural Mechanics
Department of Structural Engineering
Budapest University of Technology and Economics
H–1111 Budapest, Bertalan L. u. 2, Hungary

Abstract

This paper presents the results of an experimental study on a special type of composite connection of a thin-walled beam to concrete deck. It is applied in a light-gauge floor system that is built by thin-walled C-sections, trapezoidal sheeting as a formwork and an upper concrete deck. The self-drilling screw fastener between the sheets and the top flanges of the C-profile creates the composite connection between the steel beam and the concrete deck. In the present study this new type of shear connector is investigated by experiments.

The behaviour of the shear connectors are tested by standard push-out tests, considering several parameters: the fastening mode, the type and the geometry of screw; the arrangement of trapezoidal sheeting, the geometry of steel components and the effect of the reinforcement.

In the test programme the failure modes are observed and classified, according to the specialities of the behaviour of thin-walled structures. From the measured data, the load-displacement relationships are determined and the design values of the stiffness, resistance and ductility are calculated.

Keywords: cold-formed structures, composite floor, shear connector, self-drilling screw, push-out test.

1. Introduction

The application of light-gauge composite floor is a potentially economical solution in residential construction. In general the C-profiles form the framing and the trapezoidal sheeting – which is fastened to the flanges – provides both of the formwork and the connection with the concrete deck. The composite action is created by the shear connectors, which are embedded in concrete. Generally in the existing light-gauge composite floor systems special mechanical shear connectors are used which are formed according to the structural characteristics of thin-walled cold-formed structures. Different examples are presented in [1] and [2].

In the current study the standard self-drilling screw beam-to-sheat connection is proposed as shear connector. In order to reach higher efficiency in the composite action, the normal flange-to-sheet connection is modified by the partial drilling of the fastener, when the non-drilled part and the head of the screw are embedded in concrete. In the Lindab*Floor* light-gauge floor system – developed by the cooperation of Department of the Structural Engineering, TUB, and Lindab Ltd –

this type of connection is used. The structural arrangement of the floor system is illustrated in *Fig. 1*.

In the lack of information on the behaviour of this type of connection, a pilot experimental programme is completed with the purpose to determine the behaviour and the efficiency of the different connection types [3]. In the study the classical push-out test arrangement for composite connection is used, with the pertinent changes due to the structural characteristics. On the basis of the first results a proper connection type is chosen for the application in the developed floor structures and additional tests are done with further parameters.

In the paper the details and results of the experimental programme are discussed with a focus on the observed behaviour modes and their design characteristics.

2. Experimental Programme

Althogether 42 standard push-out tests are completed in two experimental programmes: pilot tests (12 specimens) and an extended, parametric test programme (30 specimens). The experimental arrangement and the test specimens are shown in *Fig. 2*. In all cases C-profile with 200 mm depth and concrete deck of 50 mm thickness with normal quality are applied.

In the pilot test programme the efficiency of the different connector elements and the fastening modes are studied, as shown in *Table 1*. The type of C-profile (C200-1.5) and the fastening mode of the trapezoidal sheeting (LTP45 with 45 mm height and 0.5 and 0.7 mm thickness), are shown in *Fig. 2*.

The applied connector elements are: two different products of standard self-drilling screw (SFS SD6-6.3, HS-6.3) and a special product (SFS SXC5-5.5, applied for sandwich panels) are used.

Two specimens are formed by normal fastening, i.e. the self-drilling screw is drilled in standard way, fully into the sheets and the flange of the C-profile. Further two specimens are completed with the so-called inverse fastening, i.e. the screw is drilled from inside of the flange so that only the threaded part of the screw is embedded in the concrete. The other specimens are formed by partial drilling: i.e. a part of the screw and the head are also in concrete. This mode is analogous to the welded headed stud in composite structures with hot rolled steel sections. The embedment length ranges from 30 to 60 mm as shown in *Table 1*.

In the further 30 specimens C200 profile with 1.5, 2.0 and 2.5 mm thickness and LTP20 trapezoidal sheeting are applied, as shown in the figure. The placing type of the trapezoidal sheeting is changed: in the positive arrangement the concrete fills the larger, and in negative arrangement the smaller rib. On the basis of the pilot tests the EJOT-JT2-6-6.3 screw (equivalent of SFS SD6-6.3) is used as a shear connector element in most part of the specimens. The fastening mode is partially drilling and the embedment length is 35 mm in all cases.

A normal quality concrete deck of 50 mm thickness is applied above the rib

in every specimen. Twelve specimens are investigated in parallel with the pertinent full-scale beam tests [6]. These specimens are formed with a minimal reinforcement ($\phi 3.6/100$).

In the tests the load is applied by hydraulic jack, as shown in *Fig. 2.* and the relative displacement is measured between the flanges and the base plate (the longitudinal deformation of the concrete deck is neglected). The measured load and displacement data are collected and monitored by the computer measurement system.
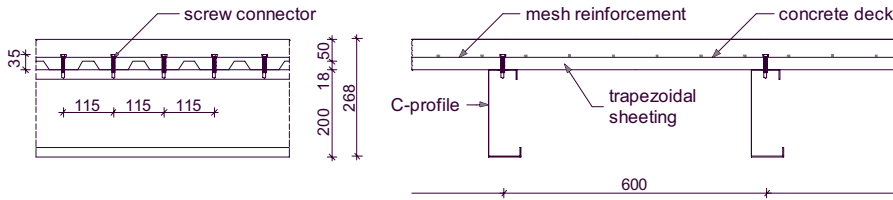
Fig. 1. Arrangement of the Lindab*Floor* cold-formed composite floor system
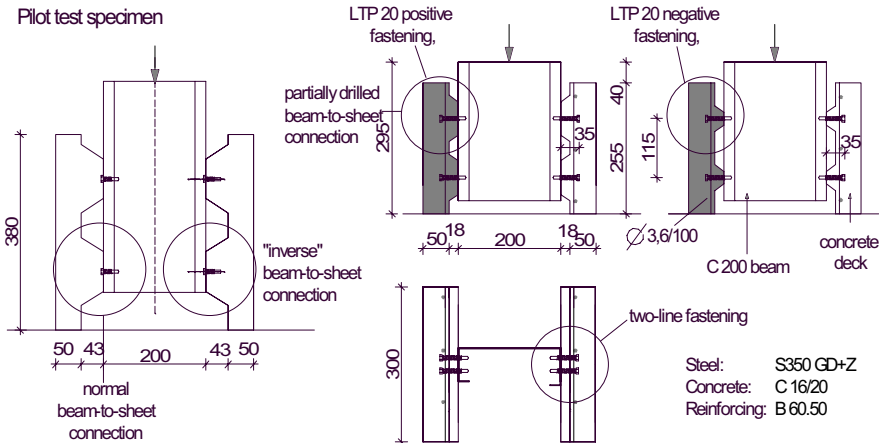
Fig. 2. Geometry of the push-out specimens

Table 1. Push-out specimens

Nr.	Notations experiments #1	Screw			Emb. length [mm]	t_{sheet} [mm]	Speci- men
		Type	Fast. mode	Line			
1.	SDn-I-s5	SF8 8D6-6.3	normal	1		0.5	1
2.	SDn-l-s7	SF5 8D6-6.3	normal	1		0.7	1
3.	SDi-l-30-s7	SF8 SDÓ-6.3	inverse	1	30	0.7	1
4.	SD1-2-30-s7	SF5 SDÓ-6.3	inverse	2	30	0.7	1
5.	HSp-I-30-s5	H8-6.3	partial	1	30	0.5	1
6.	HSp-l-30-s7	HS-6.3	partial	1	30	0.7	1
7.	HSp-I-45-s5	HS-6.3	partial	1	45	0.5	1
8.	HSp-I-60-sS	HS-6.3	partial	1	60	0.5	1
9.	HSp-2-30-s5	HS-6.3	partial	2	30	0.5	1
10.	HSp-2-60-sS	HS-6.3	partial	2	60	0.5	1
11.	SXCp-I-45-sS	SF5 SXCS-5.5	partial	1	35	0.5	1
12.	SXCp-l-55-sS	SF8 SXC5-5.5	partial	I	55	0.5	1

Nr.	Notation experiments #2	Screw		t_{beam}	Sheet fast	Reinfor- cing	Speci- men
		type	line				
13.	EJ-I-tl.5-sp	EJOT-JT2-6-6.3	1	1.5	pos	no	2
14.	EJ-1-tl.5-sn	EJOT-JT2-6-6.3	1	1.5	neg	no	2
15.	EJ-2t1.5-sp	EJOT-JT2-6-6.3	2	1.5	pos	no	1
16.	EJ-2-t1.5-sn	EJOT-JT2-6-6.3	2	1.5	neg	no	1
17.	EJ-1-t2.0-sp	EJOT-JT2-6-6.3	1	2.0	pos	no	2
18.	EJ-1-t2.0-sn	EJOT-JT2-6-6.3	1	2.0	neg	no	2
19.	EJ-2-t2.0-sn	EJOT-3T2-6-6.3	2	2.0	pos	no	1
20.	EJ-2-t2.0-sn	EJOT-JT2-6-6.3	2	2.0	neg	no	1
21.	EJ-1-t2.5-sp	EJOT-JT2-6-6.3	1	2.5	pos	no	2
22.	EJ-1-t2.5-sn	EJOT-JT2-6-6.3	1	2.5	neg	no	2
23.	EJ-2t2.5-sp	EJOT-JT2-6-6.3	2	2.5	pos	no	1
24.	EJ-2-t2.5-sn	EJOT-JT2-6-6.3	2	2.5	neg	no	1
25.	EJ-1-t1.5-sp	EJOT-JT2-6-6.3	1	1.5	pos	yes	2
26.	EJ-1-t2.0-sp	EJOT-JT2-6-6.3	1	2.0	pos	yes	2
27.	EJ-2-t2.0-sn	EJOT-JT2-6-6.3	1	2.0	neg	yes	2
28.	EJ-1-t2.5-sp	EJOT-JT2-6-6.3	1	2.5	pos	yes	1
29.	SX-1-t2.0-sp	SFS SXC5-5.5	1	2.0	pos	yes	2
30.	SX-2-t2.0-sp	SFS SXC5-5.5	2	2.0	pos	yes	2

1/a: pull-out and
pull-over

1/b: pull-out from
concrete

1/c: pull-out from the
beam flange

3..6 mm

3..6 mm

> 6 mm
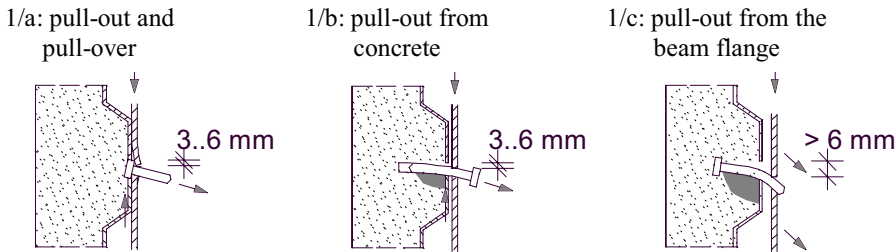
Fig. 3. Pull-out failure modes

3. Test Results

3.1. Failure Modes

On the basis of the test results the behaviour of the different composite connections are characterized by the different failure modes, as follows:

3.1.1. Pull-out failures

In the tests three basically different types of pull-out failure modes are observed, as shown in *Fig. 3*. *Pull-out and pull-over failure* (1/a) occurs when the common beam-to-sheet connection is applied. Since only the head of the screw is embedded, under relatively low force level the head pulls out from concrete. The stiffness is relatively low and the ultimate strength is approximately equivalent to the ultimate shear force of the beam-to-sheet connection without concrete. The dominancy of the steel components appears in the descending branch of the behaviour: after the ultimate load level is reached, a plastic zone appears in plates and the pull over failure occurs.

The importance of the test with the common beam-to-sheet connection is the studying of the composite effect of only the beam-to-sheet connection without concrete – for example in light-gauge floors with dry system – what is generally neglected. The experimentally determined stiffness and resistance of this connection provides the basis for the further comparisons. More information about this connection is presented in [3].

Pull-out of the screw from the concrete (1/b) is observed when the strength of the concrete is sufficient but the embedment is not effective. It is experienced in case of the 'inverse' fastening, when the bolt of the screw pulls out from concrete, as detailed in [3].

The third type of the pull-out failures is when *the fastener pulls out from the flanges* (1/c). When the displacement capacity of the screw is relatively large, the relative displacement between the concrete deck and the flanges can be sufficient.

Due to the relatively large displacement the screw rotates and becomes more and more tensioned. If the displacement capacity of the screw is high enough, the screw can pull out from the flanges before the failure of either component.

3.1.2. Screw Failures

Screw failure occurs when the embedment is effective and the strength of the concrete is relatively higher than the strength of the screw, as illustrated in *Fig.4*. Two types of this failure mode are experienced depending on the displacement capacity of the screw. If it is relatively low the ultimate failure is the *dominant screw shear* (2/a).

If the displacement capacity of the screw is relatively high, the rotation of the screw may occur – as shown in *Fig. 4* – and the screw becomes tensioned. Depending on the displacement capacity of the screw the final failure is a *combination of shear and tension* (2/b), or *dominant tension* (2/c) failure.
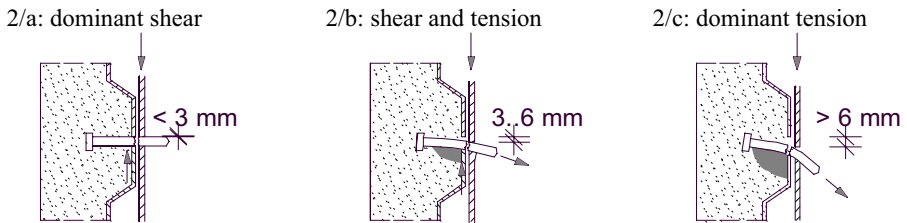
Fig. 4. Screw failure modes

Fig. 5. Concrete failure modes

3.1.3. Concrete Failure

Concrete failure occurs when the strength of the screw is relatively higher than the strength of the concrete, as shown in *Fig. 5*. Depending on the direction of the transmitted force from the connection, shear or tension type failures are observed. If the relative displacement capacity is relatively low the concrete deck *fails by the effect of shear forces* (3/a), with concrete cone failure surface and/or with a longitudinal shear crack.

If the displacement capacity of the screw is relatively high the screw and also the concrete become tensioned and the final failure is the *tension failure of the concrete deck* (3/b). The failure surface is also a crack cone similar to the shear failure. This behaviour results in the largest displacement capacity, similar to the dominant tension failure of the screw (2/c).

The dimension of the crack cone highly depends on the geometry of the rib. Narrow crack cone is observed when LTP20 trapezoidal sheeting with positive fastening mode is applied. Due to the relatively large dimensions of the rib the behaviour is similar to a deck without rib. The failed deck can be seen in *Fig.6a*.

In case of negative fastening, the crack surface is a common cone with app. 45 degrees as shown in *Fig. 6b*. It has relatively large extension when two-line fastening is applied.

In *Fig. 6c* a combined failure mode is shown: the upper connection fails by the pull-out of the screws from the flanges (1/c) and the lower connection fails by the tension of the concrete (3/b).

a)   b)   c)
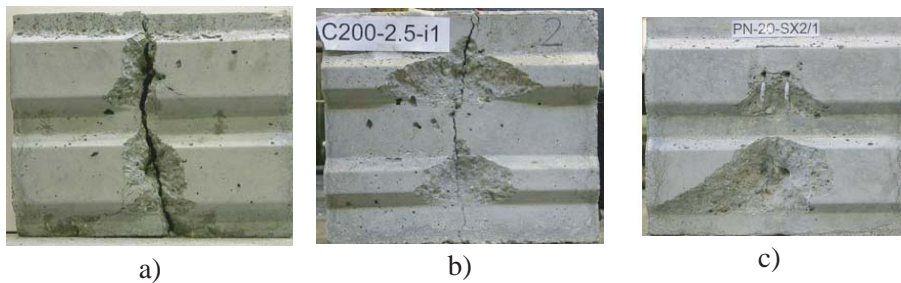
Fig. 6. Different failure surfaces of the concrete deck, a) Narrow crack cone, b)Normal
crack cone,c)Combined failure mode

3.2. Design Characteristics

Based on the measured load-displacement diagram the design values of the composite stiffness and strength can be determined. Based on the Eurocode 4 [4] and

Eurocode 3 [5] recommendations, the design value of the strength can be determined from Eq. (1):

$$P_{Rd} = (f_u/f_{ut})\frac{P_{Rk}}{\gamma_{Mv}} \tag{1}$$

where

$P_{Rk} = 0.9 \cdot P_{\text{failure,min}}$ the characteristics value of strength,

f_u the design value of the ultimate strength of the shear connector,

f_{ut} the measured ultimate strength of the shear connector in the specimen,

$\gamma_{Mv} = 1.25$ the partial safety factor.

Since in the behaviour both the steel and the concrete components have their roles, the applied approximate value of f_u/f_{ut} is given between 0,8 (for steel) and 0,85 (for concrete). Consequently the design value of the strength is given by *Eq.* (2):

$$P_{Rd} = 0.75 \cdot P_{\text{failure,min}}/\gamma_{Mv}. \tag{2}$$

On the basis of [6] proposal the force level belonging to the serviceability limit state (SLS) can be calculated by Eq. (3):

$$P_{ser} = 0.70 \cdot P_{Rd} \tag{3}$$

The stiffness is given by a secant stiffness belongs to SLS value of the load as it is shown in *Fig. 7*.

Table 2 summarizes the design values and the failure modes of the specimens. In case of two equivalent specimens the results belonging to the lowest stiffness value are shown (Nr. 13-14, 17-18, 21-22 and 25-30.).

4. Evaluation of Test Results

4.1. Stiffness

The measured stiffness values in *Table 2* show large scatter: range from 3000 to 16000 kN/m. The highest stiffness values are observed in case of connections with relatively small displacement capacity.

In the design based on the measured relatively low stiffness, the connection of the light-gauge floor beams should be considered as partial shear connection.

4.2. Resistance

The experienced ultimate load highly depends on the geometry of the connection and it has strong relationship with the observed failure modes.

With the increasing of the *thickness of the flanges* the resistance significantly increases. The thin-walled flange forms the fixing of screw and the stiffness of the fixing depends on the thickness. The measure of growth ranges from 2 to 31%. In case of two-line connections the effect of the thickness is relatively lower (see the pertinent values in *Table 2*).

The effect of the *dimensions of the rib* on the failure mode is described in Section 3.1. When positive fastening with LTP20 trapezoidal sheeting is used, the ultimate load is in most cases higher than in case of inverse fastening. It is caused by the large geometrical difference between the two types of concrete-filled ribs.

One of the important parameters is the *existence of the reinforcement*. When the described minimum reinforcing is applied, the resistance is increased by 17 to 61%. In the load-displacement diagrams of *Fig. 8* the results of 2.0 mm flange thickness and different connection arrangements are shown. The significant effect of the reinforcement can be clearly seen (curve *a* and *b*).

The *applied screw type* highly influences the resistance. As it is described in Section 3.1 if a screw with relatively large displacement capacity is applied, a favourable failure mode occurs with relatively higher resistance. This phenomenon is well illustrated in the curves of *Fig. 8*: the difference between the equivalent connections with different screw types is 23 % (curves *b* and *d*). In the first case (curve *b*) the combination of screw shear and tension, and in the second case (curve *d*) concrete tension and screw pull-out from flanges occurred.
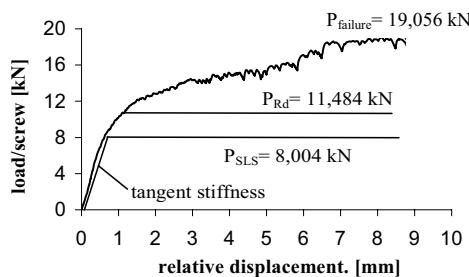
Fig. 7. Determination of design values

4.3. Ductility

In the experimental programme there is a very strong relationship between the displacement capacity and the observed failure mode. In case of shear failure of the screw or the concrete, the measured displacement capacity of the connection is relatively low (under 3 mm). When the displacement capacity of the screw allows

the rotation to some degree, the combination of shear and tension failure occurs with medium displacement capacity (between 3 and 6 mm).

The specimens, which fail by dominant tension failure, have the largest displacement capacity (over 6 mm). In accordance with Eurocode 4 [4] if the relative displacement of the connection is over 6 mm the plastic design formulas can be applied in design. The highest ductility is shown by the connections with SXC screws (d and e curves in *Fig.* 8). The displacement capacities belonging to each failure mode are shown in *Figs.* 3-5.
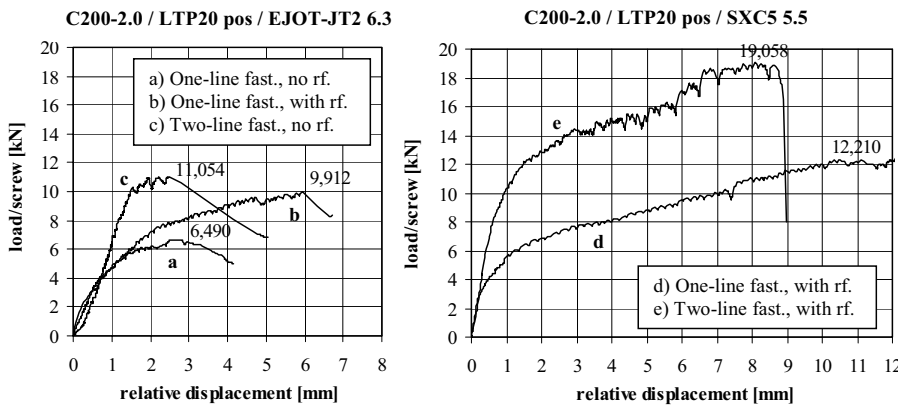
Fig. 8. Load-displacement curves of specimens with 2.0 mm flange thickness

5. Conclusions

In this paper a new type of light-gauge composite connection is studied by the application of self-drilling screw. The investigation is performed by standard push-out tests, with varying several connection parameters.

On the basis of the research the following conclusions can be drawn:

The behaviour is essentially influenced by the application of thin-walled elements.

New failure modes are observed compared with the classical composite structures with hot-rolled section.

The failure modes are identified, characterized and the connections with different parameters are classified accordingly.

The resistance and the ductility of the connection basically depend on the type of the ultimate behaviour. Consequently the connection in floor structures should be formed with connection type which shows a favourable ultimate behaviour.

Based on the experimentally measured load-displacement relationship the stiffness and the resistance of the connection are calculated in accordance with Eurocode 4 [4] and Eurocode 3 [5] recommendations.

Table 2. Design characteristics of test specimens

Nr.	Notation	Reinf.	P_{max} [kN]	P_{Rk} [kN]	P_{Rd} [kN]	P_{haszn} [kN]	SLS $stiffn.$ [kN/m]	max displ. [mm]	Failure mode
1.	SDn-1-s5	no	5.307	3.980	3.184	2.229	4500	3.32	1/a
2.	SDn-1-s7	no	5.871	4.403	3.523	2.466	*n.a.*	n.a.	1/a
3.	SDi-1-30-s7	no	9.107	6.830	5.464	3.825	7400	2.21	1/b
4.	SDi-2-30-s7	no	12.517	9.388	7.510	5.257	7400	1.97	3/a
5.	HSp-1-30-s5	no	7.546	5.660	4.528	3.169	7700	1.22	2/a
6.	HSp-1-30-s7	no	7.186	5.390	4.312	3.018	15500	1.92	2/a
7.	HSp-1-45-s5	no	7.588	5.691	4.553	3.187	17000	0.94	2/a
8.	HSp-1-60-s5	no	7.575	5.681	4.545	3.182	*n.a.*	n.a.	2/a
9.	HSp-2-30-s5	no	12.45	9.338	7.470	5.229	16400	0.99	2/a
10.	HSp-2-60-s5	no	16.494	12.371	9.896	6.927	16200	3.12	2/b
11.	SXCp-1-45-s5	no	10.053	7.540	6.032	4.222	14600	4.52	2/b
12.	SXCp-1-55-s5	no	10.614	7.961	6.368	4.458	25000	3.7	2/b
13.	EJ-1-t1.5-sp	no	6.489	4.867	3.894	2.726	7200	6	3/a
14.	EJ-1-t1.5-sn	no	4.882	3.662	2.930	2.051	5100	1.68	3/a
15.	EJ-2-t1.5-sp	no	11.472	8.604	6.883	4.818	8800	2.22	2/b
16.	EJ-2-t1.5-sn	no	8.235	6.1763	4.941	3.459	8600	1.12	3/a
17.	EJ-1-t2.0-sp	no	6.614	4.961	3.969	2.778	6500	2.5	3/a
18.	EJ-1-t2.0-sn	no	6.584	4.938	3.950	2.765	6300	4.24	3/a
19.	EJ-2-t2.0-sp	no	11.054	8.2905	6.632	4.643	*n.a.*	n.a.	3/a
20.	EJ-2-t2.0-sn	no	7.993	5.9948	4.796	3.357	6000	1.19	3/a
21.	EJ-1-t2.5-sp	no	8.075	6.056	4.845	3.391	5200	3.23	3/a
22.	EJ-1-t2.5-sn	no	5.483	4.112	3.287	2.303	4400	1.5	3/a
23.	EJ-2-t2.5-sp	no	13.361	10.021	8.017	5.612	5300	1.52	3/a
24.	EJ-2-t2.5-sn	no	8.429	6.3218	5.057	3.54	5700	1.29	3/a
25.	EJ-1-t1.5-sp	yes	7.614	5.711	4.568	3.198	3000	5.8	2/b
26.	EJ-1-t2.0-sp	yes	9.912	7.434	5.947	4.163	5200	6	2/b
27.	EJ-1-t2.0-sn	yes	6.702	5.027	4.021	2.815	11000	7	2/c
28.	EJ-1-t2.5-sp	yes	13.008	9.756	7.805	5.463	10000	7	3/b
29.	SX-1-t2.0-sp	yes	12.21	9.158	7.326	5.128	6000	10	1/c and 3/b
30.	SX-2-t2.0-sp	yes	19.056	14.292	11.434	8.004	11000	8	1/c and 3/b

The results can directly be used in calculation models which will be reported in subsequent papers.

Acknowledgement

References

[1] MUJAGIC, J. R. U. – EASTERLING, W. S. – MURRAY, T. M., Standoff Screws as Shear Connectors for Composite Trusses: Push-out Test Results and Analysis, *Proc. of the International Conference on Connection between Steel and Concrete*, Stuttgart, September, 2001, pp. 1240–1249.

[2] LAWSON, R. M. – POPO-OLA, S. O., – VARLEY, D. N., Innovative Development of Light Steel Composites in Buildings, *Proc. of the International Conference on Connection between Steel and Concrete, Stuttgart*, September, 2001, pp. 1382-1391.

[3] ERDÉLYI, SZ. – DUNAI, L., Experimental Study on Connection of Composite Light-gauge Floor System, *Proc. 3rd European Conference on Steel Structures, Coimbra, Portugal*, 2002, pp. 441–450.

[4] Eurocode 4 – Design of Composite Steel and Concrete Structures, Part 1. General Rules and Rules for Buildings, Annex 10, 1994.

[5] Eurocode 3, Design of steel structures, Part 1. General Rules and Rules for Buildings, 1993.

[6] WANG, Y. C., Deflection of Steel-concrete Composite Beams with Partial Shear Interaction, *ASCE Journal of Structural Engineering*, 1998, **124**, No. 10, pp. 1159–1165.